

Measuring rotational diffusion of MHC class I on live cells by polarized FPR[☆]

David R. Fooksman^{*}, Michael Edidin¹, B. George Barisas

Department of Chemistry, Colorado State University, Ft. Collins, CO 80523, United States

Received 16 May 2007; received in revised form 26 June 2007; accepted 26 June 2007

Available online 6 July 2007

Abstract

Clustering of membrane proteins is a dynamic process which can regulate cellular function and signaling. The size of receptor and other membrane protein clusters can in principle be measured in terms of their rotational diffusion. However, in practice, measuring rotation of membrane proteins of live cells has been difficult, largely because of the difficulty of rigidly attaching reporter groups to the molecules of interest. Here we show that polarized photobleaching recovery can detect rotation of membrane proteins genetically tagged with yellow fluorescent protein, YFP. MHC class I molecules were engineered with a rigid, in-sequence, YFP tag followed at the C-terminus by a pair of crosslinkable domains. When crosslinker was added we could detect changes in rotational anisotropy decay consistent with clustering of the MHC molecules. This result points the way to use of engineered fluorescent fusion proteins to measure rotational diffusion in native cell membranes.

© 2007 Elsevier B.V. All rights reserved.

Keywords: MHC class I; Clustering; pFPR; Anisotropy; Rotational diffusion; FRAP

1. Introduction

Clustering of membrane proteins plays an important role in cell function, particularly in signaling [1]. Receptors such as Epidermal (EGFR) and Fibroblast Growth Factor Receptors (FGFR), Fc-receptors and T and B-cell receptors require homoclustering, or clustering with co-receptors, for efficient activation and signaling [2–5]. In many other cases, the threshold for signaling is maintained by the state of oligomerization of the receptor. For example, T-cell receptor clustering plays an important role in specificity and sensitivity for antigen [6,7]. This sort of behavior is likely to be quite general [8]. Therefore, in order to understand the regulation and function of a membrane receptor, it is important to elucidate its state of oligomerization.

We are interested in using Polarized Fluorescence Photobleaching Recovery (pFPR) to measure clusters of Major Histocompatibility Complex (MHC) class I molecules. These type I membrane integral proteins are organized in clusters on the cell surface. MHC I molecules cluster through interactions with free heavy chains that seem to aggregate intact molecules on cell surfaces [9]. The addition of excess beta-2-microglobulin induces a reduction in clustering and also leads to reduced lysis by cytotoxic T-cells [10]. Depletion of membrane cholesterol also increases MHC clustering and this enhances antigen presentation to T-cells [11]. These results show that extent of MHC clustering is important for its recognition by T-cells.

Accurately measuring clusters of membrane proteins *in vivo* is technically challenging. Though a variety of quantitative microscopy techniques can detect changes in molecular clustering, these techniques do not readily measure cluster size, especially in living cells. For example, clusters can be counted and measured from confocal or total internal reflection fluorescence (TIRF) images, but many smaller clusters are lost in the resolution limit of the light microscope [11,12]. Fluorescence photobleaching recovery (FPR or FRAP) can be used to measure translational diffusion and can report on clusters smaller than the resolution of light used. However, with FPR, the diffusibility of clusters may be impeded by compartmentalization by the

[☆] This work was funded by grants from the NIH to M.E. (AI-14584, GM058554) and B.G.B. (MCB 0315798) and from the NSF to B.G.B. (MCB 0315798).

^{*} Corresponding author. Present address: Skirball Institute for Biomolecular Medicine, NYU School of Medicine, New York, NY 10016, United States. Tel.: +1 212 263 3208.

E-mail address: fooksman@saturn.med.nyu.edu (D.R. Fooksman).

¹ Present address: Department of Biology, Johns Hopkins University, Baltimore, MD 21218, United States.

membrane skeleton or by interaction with immobile species [13]. Also, the relationship between diffusion and size is not clear. Classically, lateral diffusion (D_{lat}), as defined by Saffman and Delbrück (S–D) has been related to radius (R) of the complex as $D_{\text{lat}} \propto 1/(\ln R)$ [14]. But more recently other groups have suggested $D_{\text{lat}} \propto 1/R$ [15] or $D_{\text{lat}} \propto 1/R^2$ [16].

In contrast to the uncertainties of lateral diffusion measurements, rotational diffusion (D_{rot}) provides a sensitive measure of cluster size; $D_{\text{rot}} \propto 1/(R^2)$ [14]. Rotational correlation times (RCT) for transmembrane proteins are typically 10–100 μs [17,18]. This time-scale is not readily probed by fluorescence, since the lifetimes of typical fluorophores are typically 1–10 ns. To obtain rotational kinetics in the microsecond range, investigators have typically employed time-resolved phosphorescence anisotropy (TPA) measurements to determine an RCT (see, for example, [19,20]. Phosphorescent probes, such as eosin, have long lifetimes, sometimes approaching 1 ms. However, their poor quantum yield lowers the sensitivity of TPA so that large samples are required; the method cannot be used for single cells.

TPA is thus most effective when reporting RCT smaller than ~ 1 ms. pFPR and fluorescence depletion anisotropy measurements have been used to measure slower rotation [21]. pFPR depends on the fact that anisotropy of a fluorescent probe, even if its lifetime is short, will report on the rotation of the larger molecule if the probe is rigidly associated with the larger molecule. Several groups [22,23] pioneered pFPR in a microscope-based system. In live cells, pFPR has been used only by Axelrod and colleagues [24,25] to measure rotational diffusion of acetylcholine receptors in living cells. In order to detect rotation, they used Fab fragments of immunoglobulin conjugated with eosin as phosphorescent probes, and they were able to detect microsecond changes in RCT.

We have previously shown that fusion of MHC proteins with green fluorescent protein (GFP) inserted into the protein can be used for anisotropy imaging [26]. The original constructs were partly disrupted by insertion of GFP into the sequence between the third exodomain of MHC I and the transmembrane region. We reasoned that yellow fluorescent protein (YFP) in the C-terminal, cytoplasmic, region of the MHC molecule, would not disrupt the overall structure, and could act as a rigid reporter for pFPR if the C-terminal sequence was extended beyond the fluorophore. In this paper we used a new set of MHC fusion proteins rigidly tagged with visible fluorescent protein tags as our anisotropy probes. These require no Fab labeling and can even be used to probe intracellular membranes. We believe there is a correlation between MHC organization and T-cell recognition. Our long-term goal is to generate various MHC cluster sizes and measure these sizes by rotation of our probes embedded in the aggregates.

2. Materials and methods

2.1. Constructs and sample preparation

Mouse L-cells (ATCC CCL 1.3) were grown in RPMI 1040 with 20 mM Glutamine and 10% heat-inactivated FBS. Cells were transfected with the various DNA plasmids using Fugene

6 (Roche) or by electroporation (BTX, Hawthorne, NY), following the manufacturer's protocol and used for experiments two days later. Kb-YFP and Kb-1BP have been described [11,27]. Kb-2BP was constructed in a manner similar to Kb-1BP. The 2BP binding domains were excised from the pC4M-F_v2E using XbaI and BamHI enzymes. The fragment was inserted inframe, downstream of the Kb-YFP construct. All constructs were confirmed by DNA sequencing. For crosslinking the Kb-1BP and Kb-2BP fusion proteins, excess media was removed from wells, and cells were treated with AP20187 (Ariad Pharmaceuticals, Cambridge, MA) at a final concentration of ~ 10 nM for 2 h. For live cell imaging, coverslips were washed and mounted in phosphate buffered saline (PBS) with 1% fetal bovine serum (FBS). All measurements were carried out at 25 °C.

2.2. pFPR microscope setup and equipment

A diagram of our apparatus for pFPR measurements is shown in Fig. 2. This is based on the “pump and probe” method described by Velez and Axelrod [23] with modifications. A 10 W Argon laser (Coherent Inc., Santa Clara, CA) provided a vertically-polarized 1 W output at 488 nm. The beam was split into probe and pump (bleach) beams using an unsilvered beam splitter to reflect the probe beam. The pump beam path contained a Uniblitz (Vincent Associates, Rochester, NY) shutter, controlled by the data acquisition program. The polarization of the probe beam was rotated, as needed, by a Fresnel rhomb. The probe and pump beams were recombined at a second unsilvered glass plate. The two reflections off uncoated glass surfaces reduced the probe beam strength to 0.3–1% of the pump beam. Additional neutral density filters were placed in the probe beam path as needed. A periscope was used to control position and direction of the laser beam entering into the microscope, a Zeiss Universal microscope where a dichroic beam splitter directed excitation light into a Leitz 50 \times 1.0 NA water immersion objective. The final polarization of the pump beam at the sample was horizontal. The dichroic reflector directed fluorescence from the sample through a side-port. Fluorescence passes through a photomultiplier tube (PMT) shutter and polarized components are separated by a Moxtek polarizing beam splitter (Orem, UT). Two PMH-100 photon counting PMT modules (Becker & Hickl, Berlin, Germany) collected vertically-and horizontally-polarized fluorescence, simultaneously.

Control signals for the bleach and PMT and counting of photon events registered by the PMTs were provided by a KPCI 3140 counter-timer card (Keithley Instruments, Cleveland, OH) controlled by a custom data acquisition and analysis program written using LabView 7.0 (National Instruments). PMT data were collected at rate of 2 ms/pt and displayed online together with the apparent intensity and anisotropy functions. Two-channel count rates were saved as .csv files and anisotropy and intensity re-calculated off-line using Excel (Microsoft, Redmond, WA). Anisotropies were calculated as previously described [26] using the ratio of vertically to horizontally-polarized pre-bleach light intensities to determine a g-factor. Data were fit by non-linear least squares to a single exponential decay using Prism 4.0 (GraphPad, San Diego, CA).

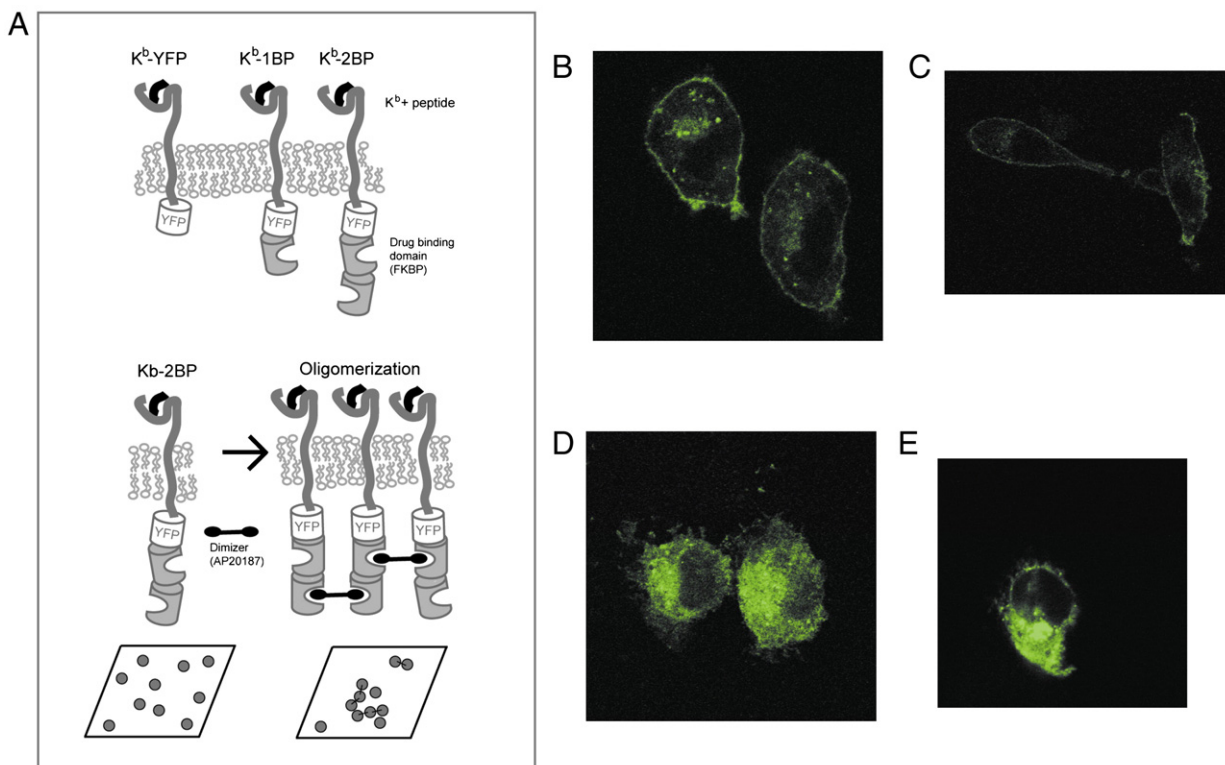


Fig. 1. 2BP Construct oligomerizes upon addition of AP20187 drug. A. The fusion constructs, Kb-YFP, Kb-1BP and Kb-2BP, used in the study are diagramed. These consist of the H2-Kb heavy chain tagged with YFP and the addition of one or two drug binding domains on the cytosolic c-terminus. Treating cells expressing the 2BP- (or 1BP-) fusion proteins with the divalent ligand, AP20187, can crosslink the cytoplasmic domains of these proteins, inducing dimers and oligomers in the cell, as modeled. L-cells were transfected with 2BP (two examples in B,C). Upon a 2 h incubation of cells with AP20187, redistribution of fluorescent protein was observed consistent with crosslinking (two examples in D,E).

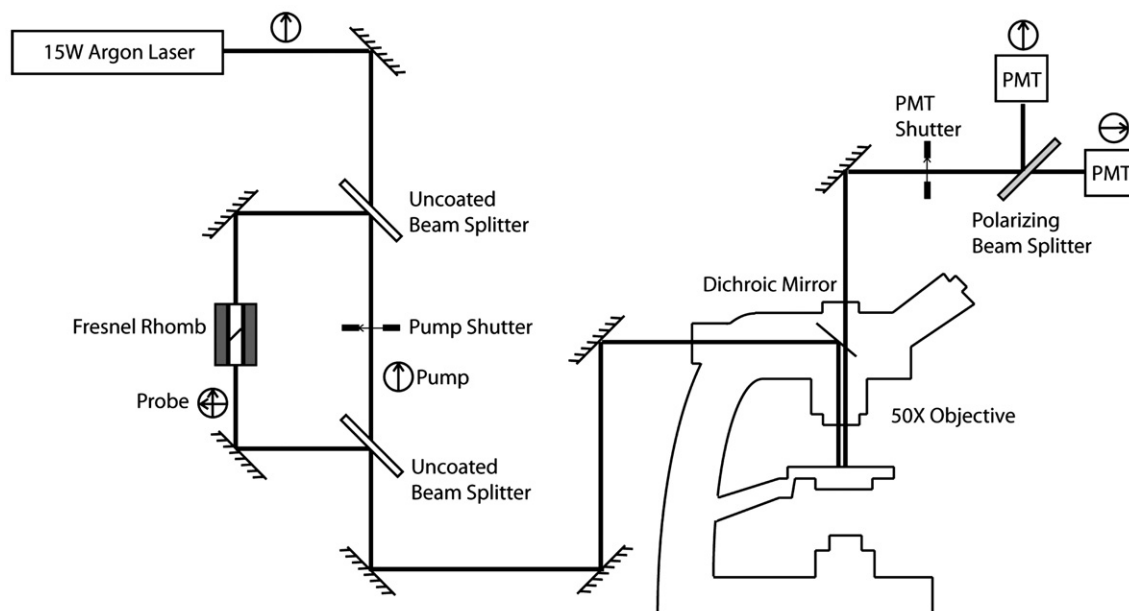


Fig. 2. Schematic diagram for pFPR setup. The components and light path are diagramed above for the pFPR setup. The probe and pump beams are labeled. The arrows indicate the polarization of the light at the various positions, vertical, horizontal, and unpolarized. For a detailed description of components, refer to the Materials and methods section.

2.3. Confocal and FPR microscopy

For confocal images, cells were fixed in 4% neutral paraformaldehyde, washed with PBS, and mounted. Confocal microscope images were taken on a Zeiss LSM510 Meta with a 63X oil objective with appropriate YFP filters, PMT detector and resolution settings. Settings were kept constant for all images. Traditional FPR measurements of lateral diffusion in live cells were taken on a modified Zeiss Axiovert, described previously [13]. A 488 nm argon laser was focused to a spot size of $\sim 0.6\text{--}0.8\ \mu\text{m}$ diameter. The beam was attenuated for sampling and bleached for 8 ms. Fluorescence recovery was measured in terms of diffusion coefficient and percent recovery to the pre-bleach level, or mobile fraction.

3. Results and discussion

To study the role of clustering on antigen presentation, we constructed several crosslinkable fusion proteins based on the

MHC I heavy chain. We used the mouse MHC allele H2-K^b C-terminally-tagged with YFP (Kb-YFP) or with one or two additional binding domains, Kb-1BP or Kb-2BP, respectively (Fig. 1A). These binding domains, as well as the ligand, AP20187, a synthetic analog of FK506, were provided by Ariad Pharmaceuticals (www.ariad.com). The addition of the divalent ligand to cells expressing these constructs induces dimerization of the Kb-1BP construct and oligomerization of the Kb-2BP (Fig. 1B–D). Since native MHCs cluster in the plasma membrane, we expect that crosslinking Kb-2BP will recruit both engineered and native molecules into clusters. Our previous work [11 and unpublished work] with Kb-1BP demonstrated increased clustering native MHC molecules after crosslinking Kb-1BP.

In order to use anisotropy to report on the rotation of the protein, we needed a rigid probe with a high intrinsic anisotropy. We reasoned that the 1BP and 2BP constructs would be good candidates for anisotropic probes because the YFP was embedded in the protein sequence with protein domains on either

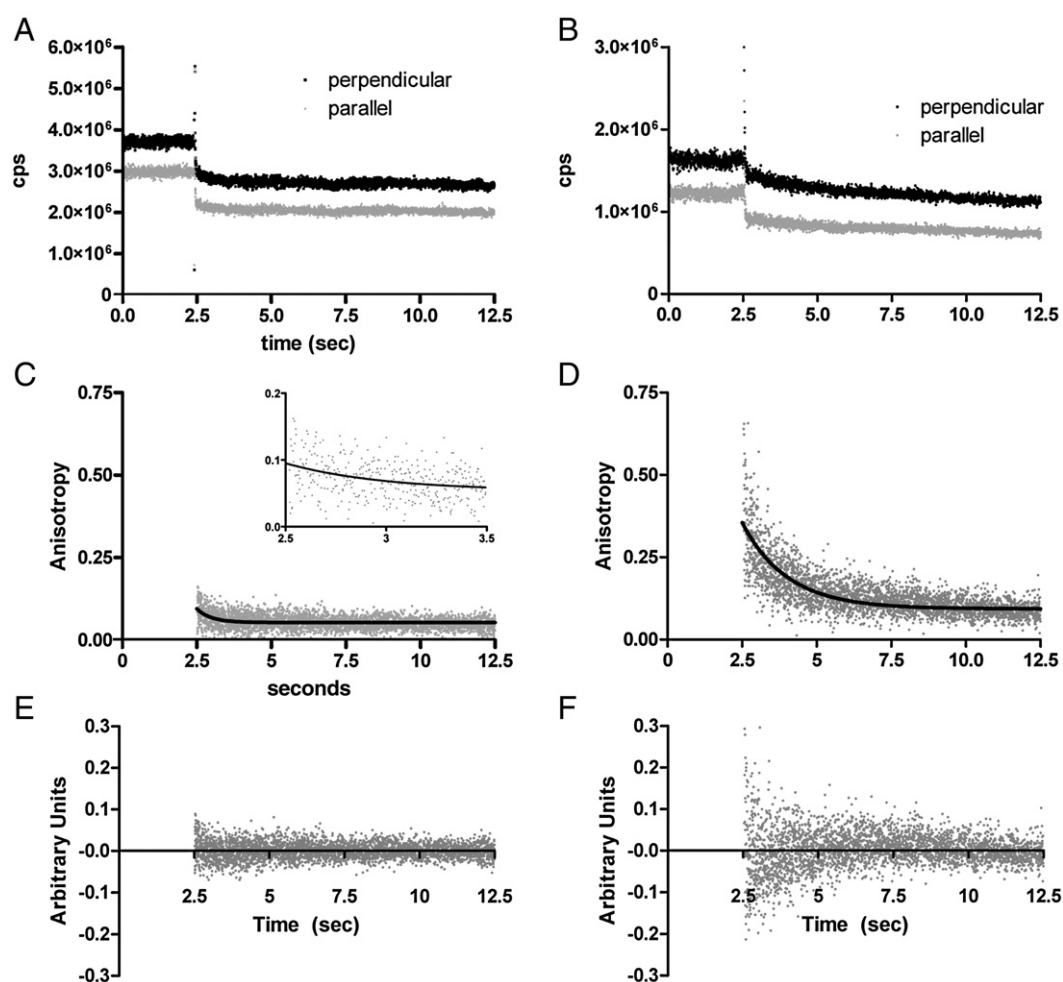


Fig. 3. Clustered 2BP exhibits slow anisotropy decay. Two datasets corresponding to measurements of single L-cells expressing 2BP on the left column and a cell expressing 2BP with AP20187 treatment on the right column. Fluorescence intensity traces from the PMTs collecting vertically polarized light, parallel to the bleach pulse, and horizontally polarized light, perpendicular to the bleach. $T=0$ corresponds to the time of bleach as shown in A and B by the decrease in fluorescence. The traces in A and B were used to calculate a depletion anisotropy in C and D, respectively. Anisotropies were fit to single exponential decays shown in the black line. Fits of 2BP untreated samples were based on only the first 500 time points due to their fast decay times (inset in C). The residuals for the fits in C and D are shown in E and F, respectively.

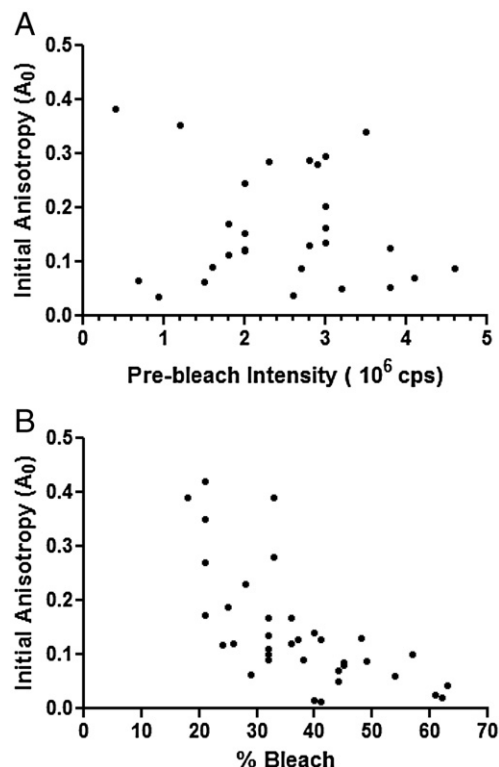


Fig. 4. Analysis of anisotropy values. Analysis of pooled data from 2BP cells treated with AP20187. In A, initial anisotropies were not sensitive to the level of construct expression as detected by YFP fluorescence intensity. However, anisotropy was correlated with amount of bleaching observed (B).

side of it. These could prevent wobbling of the fluorophore independent of the MHC molecule and so YFP anisotropy would report on the rotation of the entire tagged MHC molecule and any clusters containing it. Others have shown that GFP and its derivatives have an intrinsic anisotropy of ~ 0.33 [26]; the excitation and emission dipoles of GFP are almost parallel [28].

We used an unfocused, collimated beam to illuminate an entire cell in order to minimize the contribution of lateral mobility to fluorescence changes. We monitored polarized fluorescence using two PMTs, one for horizontally-polarized light, polarized parallel to the bleach pulse, and one for vertically-polarized light, polarized perpendicular to the bleach. Because s- and p-polarized light, that is, light polarized perpendicular and parallel to the plane of incidence, respectively, experience different reflection coefficients and phase shifts upon reflection, we opted to keep the pump (bleach) in the vertical polarization and adjusted the probe polarization so that, at the stage, the sample encountered equal intensities of horizontally- and vertically-polarized light (Fig. 2).

Two sample pFPR experiments are shown in Fig. 3. Cells were bleached with polarized light, and the recovery of fluorescence polarized parallel and perpendicular to the bleach polarization was measured. Using the two PMT traces, we calculated depletion anisotropy upon photobleaching with vertically polarized light. In Fig. 3A, L-cells transfected with 2BP, the bleaches in the vertical and horizontal channels show a similar decrease in fluorescence, which is consistent with a low initial anisotropy (Fig. 3C). However, upon treatment with the

divalent ligand, AP20187, (Fig. 3B) the parallel channel shows a greater bleach than the perpendicular channel. There is a large initial anisotropy of ~ 0.4 which decays exponentially over time (Fig. 3D).

Since these cells were transiently transfected, the number of fluorescent molecules varied from cell to cell and crowding could contribute to clustering. However, Fig. 4A, shows that there is no obvious correlation between the brightness of the cells and the anisotropy. Thus, the level of protein expression did not, by itself, induce aggregation. However, there was an inverse correlation between initial anisotropy and bleaching for 2BP cells treated with crosslinker (Fig. 4B). One factor which might cause a linkage between initial anisotropy and the preceding extent of bleaching is homoFRET between like chromophores [29]. This is plausible since YFP has good overlap between its absorption and emission spectra [30]. However, increasing extents of bleaching would decrease the likelihood that a given YFP finds another such chromophore within the Förster distance. Hence, homoFRET should decrease in more strongly bleached measurements and initial anisotropy should *increase* rather than decrease as is in fact observed. Another factor to be considered is reduction of measured initial anisotropy by extensive bleaching which causes both detector signals to

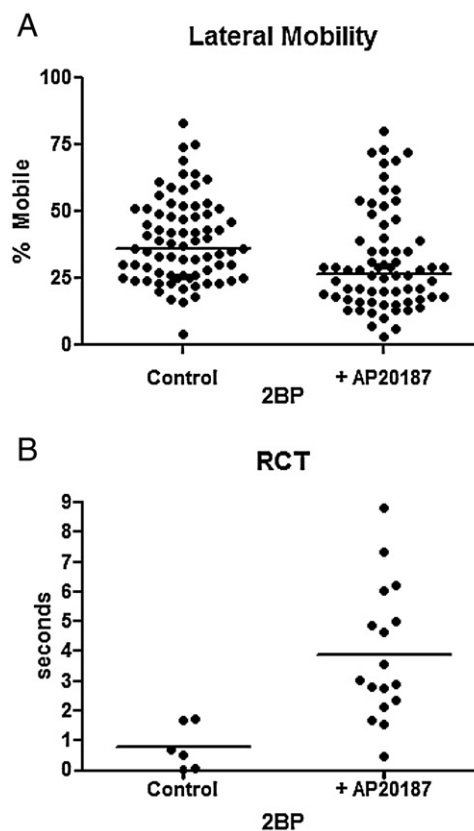


Fig. 5. Comparison of traditional and polarized FPR for measuring crosslinking. Vertical scatter plots, the horizontal lines correspond to mean values. In A, lateral mobility of 2BP+AP20187 on transfected L-cells was measured by traditional FPR. The percent recovery after photobleaching, or mobile fraction, is plotted for each condition. In B, pFPR was used to probe the rotational diffusion of 2BP molecules with and without drug. The rotation correlation times are plotted for each condition.

Table 1
Summary of pFPR results¹

	Initial anisotropy	RCT (seconds)
Kb-YFP	0.086±0.033	n/a ²
1BP	0.063±0.015	n/a ²
1BP+AP20187	0.087±0.066	n/a ²
2BP	0.111±0.072	0.769±0.312
2BP+AP20187	0.199±0.025	3.89±0.548

¹Mean values shown with standard error.

²In the case of measuring RCT, several conditions showed no detectable decay on the timescale sampled. Therefore, no RCT was available.

approach zero. However, calculations based on our experimental geometry indicate that a 70% bleach would only reduce anisotropy to 0.31, about equal to the *highest* initial anisotropies observed. Hence, while bleaching-induced saturation produces effects of the correct general type, the effects of bleaching are predicted to be much smaller than those actually encountered. The factor perhaps most likely to cause linkage between extent of bleaching and initial anisotropy is heterogeneity in size, and thus rigidity, of protein aggregates among various cells examined. If one cell exhibits substantially larger aggregates than another, then proteins in the larger aggregates will be more restricted in various wobbling motions so that their observed initial anisotropies more nearly approach the photophysical limit. Similarly, chromophores in larger aggregates should be better shielded from solution species like oxygen so that their rate of bleaching would be reduced. This possibility is supported by the fact that a linkage between extent of bleaching and initial anisotropy was observed only in treated 2BP cells, presumably the cell system exhibiting the largest MHC clusters.

Although we were able to detect the effect of crosslinking of the 2BP by measuring lateral diffusion in traditional FPR, the changes after crosslinking were more pronounced with pFPR. As shown in Fig. 5, the laterally-mobile fraction was significantly reduced from a mean of 40% to 33% ($p < 0.05$) upon crosslinking, consistent with formation of large aggregates. The lateral diffusion coefficient decreased from 2.5×10^{-9} to 2.2×10^{-9} cm²/s upon clustering. This change was not statistically significant, as expected from by the Saffman-Delbrück relation. In contrast, the changes in rotational correlation time, RCT (Fig. 5B) and in initial anisotropy (Table 1) were pronounced and statistically significant ($p < 0.004$).

We conducted similar measurements on all of our fluorescent constructs and these results are summarized in Table 1. On the time scale that we could measure, milliseconds to seconds, we were able to detect an anisotropic decay only with our 2BP construct. This suggested that the C-terminal tagged YFP had too much wobble to report on the rotation of clusters of MHC molecules. Even a YFP followed by a single binding domain, 122 amino acids, with or without dimerization did not report the RCT of the whole MHC molecule. Only the 2BP construct, YFP followed by 243 amino acids, was rigid enough to report the RCT of the engineered MHC molecule.

Although we obtained an RCT of ~0.8 s for untreated 2BP, it is likely that this overestimates the true value. On the time scale that we could resolve, data exhibited a limited decay (Fig. 3C), of about a second, starting from low initial anisotropies.

However, the RCT of a protein with two transmembrane segments is typically about 10 μ s [16]. Therefore we suspect that, if we could bleach and sample faster, we would see a larger initial anisotropies decaying with shorter RCTs than those detected here.

From the RCT we determined for crosslinked 2BP, we can estimate the cluster size. If we assume that the RCT of untreated 2BP is that of wild type MHC I, with a RCT of 10 μ s, then the aggregates rotate about 400,000-fold slower. The rotational diffusion constant of a membrane entity is proportional to the inverse square of its radius. Therefore, a 400,000-fold slowing in rotation would correspond to a ~630 fold change in radius.

Crosslinking 2BP induces substantial internalization. Thus, part of the signal we measured came from fluorescent molecules residing in internal membranes, as seen in the images in Fig. 1D–E. However, it is unlikely that fluorescence recovery is due to rotation of internal vesicles as they are tethered by cytoskeletal motors [31].

4. Conclusion

With the growing need to measure changes in lateral organization of membrane molecules, we believe these results suggest a new way to study these processes on the surface. While we were only able to detect formation of quite sizeable clusters, nonetheless we show the feasibility of measuring rotational diffusion for genetically-tagged fluorescent molecules and they demonstrate one strategy to restrain the independent rotation of the fluorescent tags. Moreover, as these probes do not require Fab labeling for imaging, they can be used to explore internal compartments without insult to the cell. Our future work will focus on enhancing the resolution of the technique to visualize smaller extents of molecular clustering that are important for physiologic function.

References

- [1] H. Metzger, Transmembrane signaling: the joy of aggregation, *J. Immunol.* 149 (1992) 1477–1487.
- [2] F. Ozcan, P. Klein, M.A. Lemmon, I. Lax, J. Schlessinger, On the nature of low- and high-affinity EGF receptors on living cells, *Proc. Natl. Acad. Sci. U. S. A.* 103 (2006) 5735–5740.
- [3] M. Gopalakrishnan, K. Forsten-Williams, M.A. Nugent, U.C. Tauber, Effects of receptor clustering on ligand dissociation kinetics: theory and simulations, *Biophys. J.* 89 (2005) 3686–3700.
- [4] B.G. Barisas, S.M. Smith, J. Liu, J. Song, G.M. Hagen, I. Pecht, D.A. Roess, Compartmentalization of the Type I Fcepsilon receptor and MAFA on mast cell membranes, *Biophys. Chemist.* 126 (2007) 30–35.
- [5] R.A. Stein, E.J. Hustedt, J.V. Staros, A.H. Beth, Rotational dynamics of the epidermal growth factor receptor, *Biochemistry* 41 (2002) 1957–1964.
- [6] R.N. Germain, T-cell activation: the power of one, *Curr. Biol.* 13 (2003) 137–139.
- [7] A.J. George, J. Stark, C. Chan, Understanding specificity and sensitivity of T-cell recognition, *Trends Immunol.* 26 (2005) 653–659.
- [8] J.N. Sachs, D.M. Engelman, Introduction to the membrane protein reviews: the interplay of structure, dynamics, and environment in membrane protein function, *Annu. Rev. Biochem.* 75 (2006) 707–712.
- [9] J. Matko, Y. Bushkin, T. Wei and M. Edidin. Clustering of class I HLA molecules on the surfaces of activated and transformed human cells, *J. Immunol.* 152 (1994) 3353–3360.701–708.

- [10] Bodnar, Z. Bacso, A. Jenei, T.M. Jovin, M. Edidin, S. Damjanovich, J. Matko, Class I HLA oligomerization at the surface of B cells is controlled by exogenous beta(2)-microglobulin: implications in activation of cytotoxic T lymphocytes, *Int. Immunol.* 15 (2003).
- [11] D.R. Fooksman, G.K. Gronvall, Q. Tang, M. Edidin, Clustering class I MHC modulates sensitivity of T cell recognition, *J. Immunol.* 176 (2006) 6673–6680.
- [12] Q. Tang, M. Edidin, Vesicle trafficking and cell surface membrane patchiness, *Biophys. J.* 81 (2001) 196–203.
- [13] J. Kwik, S. Boyle, D. Fooksman, L. Margolis, M.P. Sheetz, M. Edidin, Membrane cholesterol, lateral mobility, and the phosphatidylinositol 4,5-bisphosphate-dependent organization of cell actin, *Proc. Natl. Acad. Sci. U. S. A.* 100 (2003) 13964–13969.
- [14] P.G. Saffman, M. Delbruck, Brownian motion in biological membranes, *Proc. Natl. Acad. Sci. U. S. A.* 72 (1975) 3111–3113.
- [15] Y. Gambin, R. Lopez-Esparza, M. Refay, E. Sieracki, N.S. Gov, M. Genest, R.S. Hodges, W. Urbach, Lateral mobility of proteins in liquid membranes revisited, *Proc. Natl. Acad. Sci. U. S. A.* 103 (2006) 2098–2102.
- [16] G. Guigas, M. Weiss, Size-dependent diffusion of membrane inclusions, *Biophys. J.* 91 (2006) 2393–2398.
- [17] B.G. Barisas, W.F. Wade, T.M. Jovin, D. Arndt-Jovin, D.A. Roess, Dynamics of molecules involved in antigen presentation: effects of fixation, *Mol. Immunol.* 36 (1999) (2003) 331–339.
- [18] J. Song, G.M. Hagen, D.A. Roess, I. Pecht, B.G. Barisas, The mast cell function-associated antigen and its interactions with the type I Fcepsilon receptor, *Biochemistry* 41 (2002) 881–889.
- [19] R.H. Austin, J. Karohl, T.M. Jovin, Rotational diffusion of *Escherichia coli* RNA polymerase free and bound to deoxyribonucleic acid in nonspecific complexes, *Biochemistry* 22 (1983) 3082–3090.
- [20] T.M. Eads, D.D. Thomas, R.H. Austin, Microsecond rotational motions of eosin-labeled myosin measured by time-resolved anisotropy of absorption and phosphorescence, *J. Mol. Biol.* 179 (1984) 55–81.
- [21] T.R. Londo, N.A. Rahman, D.A. Roess, B.G. Barisas, Fluorescence depletion measurements in various experimental geometries provide true emission and absorption anisotropies for the study of protein rotation, *Biophys. Chemist* 48 (1993) 241–257.
- [22] L.M. Smith, R.M. Weis, H.M. McConnell, Measurement of rotational motion in membranes using fluorescence recovery after photobleaching, *Biophys. J.* 36 (1981) 73–91.
- [23] M. Velez, D. Axelrod, Polarized fluorescence photobleaching recovery for measuring rotational diffusion in solutions and membranes, *Biophys. J.* 53 (1988) 575–591.
- [24] M. Velez, K.F. Barald, D. Axelrod, Rotational diffusion of acetylcholine receptors on cultured rat myotubes, *J. Cell Biol.* 110 (1990) 2049–2059.
- [25] Y. Yuan, D. Axelrod, Subnanosecond polarized fluorescence photobleaching: rotational diffusion of acetylcholine receptors on developing muscle cells, *Biophys. J.* 69 (1995) 690–700.
- [26] J.V. Rocheleau, M. Edidin, D.W. Piston, Intrasequence GFP in Class I MHC molecules, a rigid probe for fluorescence anisotropy measurements of the membrane environment, *Biophys. J.* 84 (2003) 4078–4086.
- [27] E.T. Spiliotis, T. Pentcheva, M. Edidin, Probing for membrane domains in the endoplasmic reticulum: retention and degradation of unassembled MHC class I molecules, *Mol. Biol. Cell* 13 (2002) 1566–1581.
- [28] F.I. Rosell, S.G. Boxer, Polarized absorption spectra of green fluorescent protein single crystals: transition dipole moment directions, *Biochemistry* 42 (2003) 177–183.
- [29] D.S. Lidke, P. Nagy, B.G. Barisas, R. Heintzmann, J.N. Post, K.A. Lidke, A.H.A. Clayton, D. Arndt-Jovin, T.M. Jovin, Imaging molecular interactions in cells by dynamic and static fluorescence anisotropy (rFLIM and emFRET), *Biochem. Soc. Trans.* 31 (2003) 1020–1027 Part 5.
- [30] G.H. Patterson, D.W. Piston, B.G. Barisas, Förster distances between green fluorescent protein pairs, *Anal. Biochem.* 284 (2000) 438–440.
- [31] C. Kural, H. Kim, S. Syed, G. Goshima, V.I. Gelfand, P.R. Selvin, Kinesin and dynein move a peroxisome in vivo: a tug-of-war or coordinated movement? *Science* 308 (2005) 1469–1472.